PEM Fuel Cell Stack Hardware-In-the-Loop Emulation using DC/DC Converter Design

Fei Gao, *Student Member, IEEE*, Benjamin Blunier, *Member, IEEE*, Marcelo Simões, *Senior Member, IEEE*, Abdellatif Miraoui, *Senior Member, IEEE*, and Abdellah El-Moudni

***Abstract*—A model based PEM (Proton exchange membrane) fuel cell emulator with a DC/DC power converter design is presented in this paper. The presented multi-physical fuel cell stack model approaches three major domains: electrical, fluidic and thermal Where a fuel cell dynamic phenomena analysis is performed and discussed through those different physical domains. Analysis are performed on the dynamics of those three levels of emulation and a DC/DC converter is designed for the fuel cell electrical emulation purpose. An appropriate control strategy for the converter is also discussed. The emulator experimental results are validated with a commercial Ballard NEXA 1.2 kW fuel cell stack. Such an emulator is of great interest for Hardware-In-the-Loop (HiL) applications to be used for real time hardware validation of fuel cell systems.**

***Index Terms*—Fuel cell, Buck converter design, Emulation, Hardware-In-the-Loop**

I. Introduction

Fuel cells have became a very active research field today and the need of real time emulators is required for validation and studies of system integration. Compared to many other existing energy generation systems, such as internal combustion engine, the PEM (Proton Exchange Membrane) fuel cell has some significant advantages:, the fuel cell system overall efficiency can reach about 50 % [1]; the operating temperature of a fuel cell is relatively low, which leads to a faster startup, the fuel cell is environmental friendly if the hydrogen is produced from renewable or carbon free primary energy sources, the byproducts of the electrochemical reaction are only heat and water if the stack is supplied by pure hydrogen; Finally, the fuel cell stack system can be very compact when compared to other sources of energy.

Despite of such advantages, a PEM fuel cell stack itself can not be used directly as an energy supply. The fuel cell DC output voltage is highly dependent to the current which imposes a high output voltage variation. For example, for a 1.2 kW with a 47 cells stack, a current variation from 0 A to 40 A, will lead to a stack output voltage variation between 45 V and 25 V [2]. This voltage range is not acceptable for most of the DC electrical devices. Moreover, if the electrical device needs an AC supply, the fuel cell system must be connected to an inverter to provide alternating current.

One of the key challenges of fuel cell systems is the design of an appropriate power converter for power output. During the design phase, the converter needs to be tested and adjusted with the real fuel cell stack, and then it must be validated. However, design and development of systems, such as testing of compressor control, power and energy management, performance optimization may damage a fuel cell very quickly. In addition, fuel cell test cost (hydrogen consumption and the need of safety in the installations.) is still relatively high for today.

The drawbacks mentioned above support the interest of designing a PEM fuel cell model-based emulator for Hardware-In-the-Loop (HiL) real time implementation. In fuel cell system power converter design as well as in other developments, power converters can be tested and improved with the fuel cell emulator initially without any damage risks, with low cost of operation and without safety needs.

A fuel cell model based emulator requires that the output of a real stack must be reproduced accurately by the emulator. The computation time of the emulator should be in real time for HiL tests. Therefore, model complexity is a compromise between accuracy and computational speed.

Many PEM fuel cell emulators have been previously proposed [3]-[9]. A common drawback of these emulators is that the fuel cell models are too simplified and do not represent accurately all the system physics and non-linearities. Most of those works consider only the electrical system level emulation. In fact, the fuel cell is a multi-physical system and other physical domains, such as fluidic and thermal phenomena should be considered. On the other hand, the emulator power converter design must meet the fuel cell dynamics in different physical domains. This can not be done without a multi-physical fuel cell model.

The paper is organized as follows: in the next section, a one dimension multi-physical PEM fuel cell stack model is presented. This model is then implemented in the fuel cell emulator with a real-time system. After that, a fuel cell emulator structure with the DC/DC buck converter design is presented and then the experimental results are discussed.

II. Multi-physic fuel cell stack model

A multi-physical PEM fuel cell stack model used for fuel cell real-time simulation is summarized in this section. More detailed model equations with fully experimental validation are presented in [10].

F. Gao, B. Blunier, A. Miraoui and A. El-Moudni are with Transport and System laboratory (SeT), University of Technology of Belfort-Montbeliard, 90010, Belfort, France (e-mail: fei.gao@utbm.fr).

M. Simões is with Colorado School of Mines, 1610 Illinois St.Golden CO 80401-1887, U.S. (e-mail: msimoes@mines.edu).

2009 IEEE Electrical Power & Energy Conference
978-1-4244-4509-7/09/$25.00 ©2009 IEEE

A. Cell Electrical Model

The single cell voltage output can be expressed as follow:

$$V_{cell} = E - V_{act(Dynamic)} - V_{ohm} \quad (1)$$

where E is the electromotive force (V), $V_{act(Dynamic)}$ the cell dynamic activation losses (V) and V_{ohm} the cell ohmic losses (V).

The cell electromotive force is obtained from the thermodynamic formula:

$$E = 1.229 - 0.85 \cdot 10^{-3}(T - 298.15) + \frac{R \cdot T}{2F} \ln\left(\sqrt{P_{O2}} \cdot P_{H2}\right) \quad (2)$$

where T is the temperature of the layer (K), P_{O2} the oxygen pressure (atm) at the interface of cathode catalyst layer, P_{H2} the hydrogen pressure (atm) at the interface of anode catalyst layer, R the ideal gas constant (J/mol.K) and F the Faraday constant (C/mol).

In fuel cell, the electrical dynamic response to a current change is due to the "double layer capacitance phenomena" at the interface of catalyst layer. This dynamic activation loss voltage can be expressed by the following transfer function:

$$V_{act(Dynamic)} = V_{act} \Big/ \left(1 + C\frac{V_{act}}{i}s\right) \quad (3)$$

where C is the fuel cell double layer capacitance (F), i the stack current (A) and V_{act} the cell static activation losses (V).

The cell static activation losses can be calculated from:

$$V_{act} = \varepsilon_1 + \varepsilon_2 \cdot T + \varepsilon_3 \cdot T \cdot \ln\left(\frac{P_{O2}}{5.08 \cdot 10^6 \cdot e^{-\left(\frac{498}{T}\right)}}\right) + \varepsilon_4 \cdot T \cdot \ln(i) \quad (4)$$

where ε_1 to ε_4 are four empirical parameters, which need to be identified from the stack static polarization curve.

The cell ohmic losses are mainly due to the membrane resistance. This membrane resistance can be obtained by integrating the membrane local resistivity over its thickness:

$$R_{mem} = \frac{1}{S}\int_0^{\delta} r(T, \lambda(z))dz \quad (5)$$

With the expression of membrane resistivity:

$$r = \begin{cases} \dfrac{e^{\left[1268 \cdot \left(\frac{1}{T} - \frac{1}{303}\right)\right]}}{0.1933} & if \;\; 0 < \lambda(z) \le 1 \\ \dfrac{e^{\left[1268 \cdot \left(\frac{1}{T} - \frac{1}{303}\right)\right]}}{0.5193 \cdot \lambda(z) - 0.326} & if \;\; \lambda(z) > 1 \end{cases} \quad (6)$$

where $\lambda(z)$ is the membrane local water content.

The cell ohmic loss can be expressed after the Joule's law:

$$V_{ohm} = R_{mem} \cdot i \quad (7)$$

B. Cell Fluidic Model

The fluidic dynamic response of fuel cell is due to the gas pressure dynamic in fuel cell channels which are given by the mass balance:

$$\frac{M_{gas} \cdot V_{Ch}}{R \cdot T}\left(\frac{d}{dt}P_{Ch}\right) = \sum_{in/out}^{Ch} q_{fluid} \quad (8)$$

where V_{ch} is the volume of the channels (m^3), M_{gas} is the gas molar mass (kg/mol), P_{cv} is the gas pressure in the channels (Pa) and q_{fluid} is the fluid mass flow(s) (kg/s) entering or leaving the channels.

The gas pressure drop in the channels due to the mechanical losses assuming a laminar flow can be expressed by the Darcy-Weisbach Equation:

$$\Delta P = f_{darcy}\frac{\rho_{CV} \cdot L}{2D_{hydro}}{V_S}^2 \;\text{ with }\; f_{darcy} = \frac{64}{\mathrm{Re}} \quad (9)$$

where f_{darcy} is the Darcy friction factor, D_{hydro} is the hydraulic diameter of the channels (m), V_s is the mean fluid velocity in the channels (m/s), L is the length of the channel (m) and Re is the fluid Reynolds number.

The phenomenon of the gas diffusion of each species i in the gas diffusion layers (GDL) is described by the Stefan-Maxwell equation:

$$\Delta P_i = \frac{\delta \cdot R \cdot T}{P_{tot} \cdot S}\sum_{j \neq i}\frac{P_i \cdot \frac{q_j}{M_j} - P_j \cdot \frac{q_i}{M_i}}{D_{ij}} \quad (10)$$

where δ is the GDL thickness (m), S is the GDL layer section (m^2), P_{tot} is the mean gas total pressure (Pa) in the GDL layer, M is the gas molar mass (kg/mol), j stands for species other than species i, and D_{ij} is the binary diffusion coefficient between the species i and j (m^2/s).

The water balance in the membrane layer can be described by two different phenomenons: The *electro-osmosis* phenomenon in (11), and the *back diffusion* phenomenon in (12).

$$J_{drag} = \frac{n_{sat} \cdot \lambda(z)}{11} \cdot \frac{i}{2F} \cdot M_{H2O} \quad (11)$$

$$J_{back\_diff} = -\frac{\rho_{dry}}{M_n} \cdot D_\lambda \cdot \frac{d\lambda(z)}{dz} \cdot S \cdot M_{H2O} \quad (12)$$

where n_{sat}=22 is the electro-osmotic drag coefficient for maximum hydration condition, ρ_{dry} is the dry density of the membrane (kg/m^3), $D_{(\lambda)}$ the mean water diffusion coefficient in the membrane (m^2/s), and M_n the equivalent mass of the membrane (kg/mol).

The total water mass flow (kg/s) in membrane can be then expressed:

$$q_{H2O,net} = J_{drag} + J_{back\_diff} \quad (13)$$

C. Cell Thermal Model

The thermal dynamic response of fuel cell is due to the thermal capacity of each cell layer. These temperature dynamics in each layer can be generally described as:

$$\left(\rho \cdot V \cdot C_p\right)\frac{dT}{dt} = \sum Q_{heat\ flow} \qquad (14)$$

where ρ is the mean layer density (kg/m^3), V is the layer volume (m^3), C_p is the layer thermal capacity (J/kg·K) and Q stands for the different types of heat flows entering or leaving the layer: conduction, forced convection, natural convection, radiation, convective mass flow and internal heating sources (J/s).

In these heat flows, the Fourier's law is used to describe the solid heat transfer and the Newton's cooling law used to describe the fluid heat transfer (forced convection and natural convection). The internal heat sources are due to the entropy change during electro-chemical reaction, the activation losses and the resistive losses from the membrane resistance.

D. Model Experimental Validation

The model is set and validated for a Ballard NEXA air cooled 1.2 kW with a 47 cells stack which, supplied by compressed air and pure hydrogen.

The experimental stack current profile used for the model simulation is shown in Fig. 1. The comparison between the real stack responses and model predictions of stack voltage output and stack temperature variation are illustrated separately in Fig. 2 and Fig. 3.

The results show very good agreements through different physical domains. The fuel cell stack dynamic phenomena are well reproduced by the model. Thus, the model is suitable for the fuel cell emulation purpose.

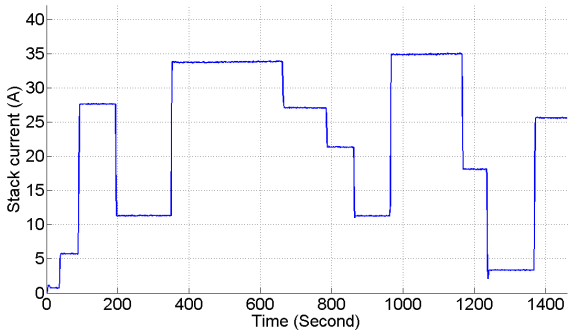

Fig. 1 Stack Current profile

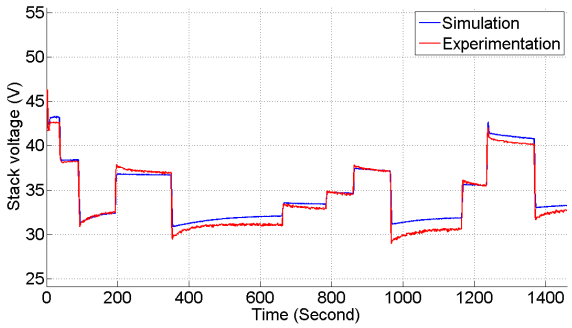

Fig. 2 Stack voltage responses (real stack and model)

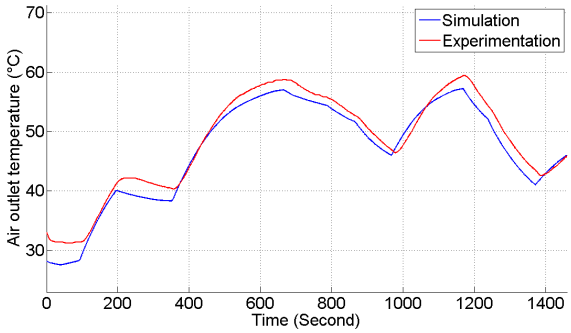

Fig. 3 Stack temperature responses (real stack and model)

The model has been developed in Matlab-Simulink programs using C based S-function calls, and implemented in a dSpace 1 GHz real-time processor. With efficient C language programming, this complex multi-physical model can run about 3 times faster than real-time (33 % of real-time processor load).

III. Fuel Cell Dymanic Phenomenas Analysis

As mentioned in the previous section, the fuel cell dynamic phenomena can be observed in three major physical domains: electrical, fluidic and thermal. The dynamic response for each domain can vary significantly at fast load current changes. However, each of them is related to different nature and the dynamic behavior is quite different. An evaluation of dynamic response has been done for a NEXA 1.2 kW fuel cell stack.

A. Electrical Dynamic: Double Layer Capacitance

From (3), the electrical dynamic time constant can be obtained:

$$\tau_{electrical} = C \cdot \frac{V_{act}}{i} \qquad (15)$$

The ratio between V_{act} and i during different stack load current change (Fig. 1) is plotted in Fig. 4.

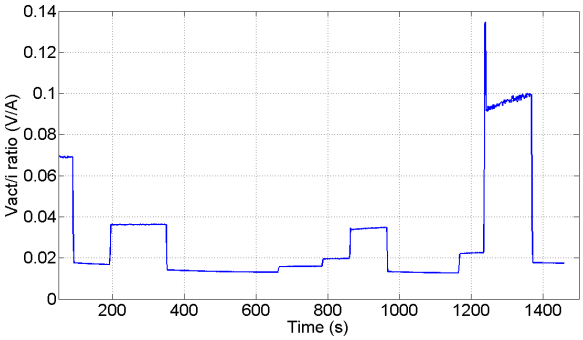

Fig. 4 V_{act} /i ratio during stack current changes

From the test results, it can be concluded that the ratio V_{act}/i value is generally between 0.01 and 0.1 (V/A). On the other hand, the fuel cell double layer capacitance can be identified through different experimental methods. A typical value range of this capacitance is between 0.01 and 5 (F) [11].

By multiplying these 2 values, the electrical dynamic time constant range can be calculated to vary from 100 µs to 500 ms.

B. Fluidic Dynamic: Channels Volumes

The fluidic dynamic in the fuel cell is generally due to the sudden flow rate changes in the gas channels, as in the case of a stack current change. The most influential parameter on fluidic dynamic is the air inlet flow rate changes during load changes in order to maintain the cathode supply stoichiometry. This dynamic leads to oxygen pressure change in the cathode gas channels, which is a very sensitive parameter for the fuel cell reaction kinetics.

The cathode gas channels pressures at different stack load currents for the NEXA stack are shown in Fig. 5:

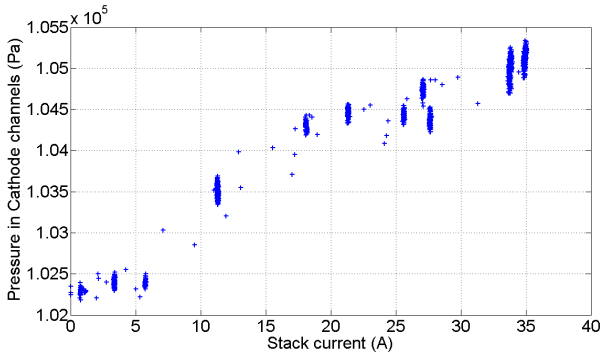

Fig. 5 Cathode channels pressures at different stack currents

Using a linear approximation, the cathode channels pressure variation per current variation can be computed:

$$\frac{\Delta P_{cathode}}{\Delta i} \approx 85.7(\mathrm{Pa/A}) \qquad (16)$$

In the NEXA system, the cathode air inlet mass flow rate is controlled by an air compressor and this flow rate is almost proportional to the stack current:

$$\frac{\Delta \dot{q}_{cathode\,air\,inlet}}{\Delta i} \approx 2.567 \cdot 10^{-5}\left(\mathrm{kg/(s \cdot A)}\right) \qquad (17)$$

From (8), (16) and (17), the fluidic channels dynamics time constant can be approximated by:

$$\tau_{fluidic\,ch} \approx \frac{\Delta P_{cathode}/\Delta i}{\Delta \dot{q}_{cathode\,air\,inlet}/\Delta i} \cdot \frac{M_{gas} \cdot V_{Ch}}{R \cdot T} \qquad (18)$$

In the case of a NEXA fuel cell stack, the stack temperature range is from 20 °C to 70 °C. Thus the fluidic channels dynamic time constant range can be calculated to vary from 3.43 µs to 4.01 µs.

C. Thermal Dynamic: Stack Thermal Capacities

The thermal dynamic response in a fuel cell is the most significant behavior due to the large stack thermal capacity. This dynamic response is given by (14). The fuel cell thermal fluxes are coming from several sources: conduction, forced convection, convective mass flow, and others. And all these thermal fluxes are also dependent on the fuel cell temperature itself. Thus, the thermal dynamic time constant of such a complex physical system is difficult to be analyzed explicitly.

However, some conclusions can still be made from the experimental data in Fig. 3. From the given stack current profile and its temperature curve, it can be reasonably concluded that the fuel cell thermal time constant is relatively high. In the case of the NEXA fuel cell stack, its value should not be lower than 10 s.

IV. Fuel Cell Stack Power Output Emulation

The fuel cell stack voltage is emulated by a controlled DC/DC buck converter connected to the real-time model.

A. Electrical Emulator Structure

The actual fuel cell emulator structure is given in Fig. 6.

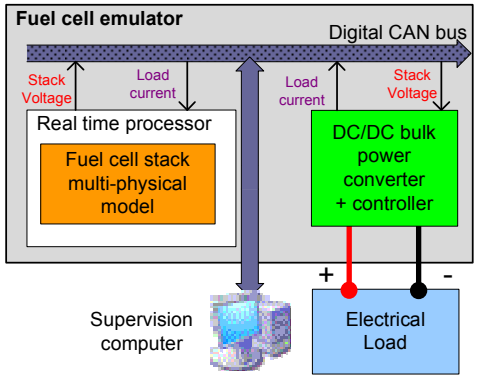

Fig. 6 Fuel cell emulator structure diagram

The fuel cell stack model implemented in the real-time processor communicates with the DC/DC buck power converter via a digital CAN (Control Area Network) bus. The converter is connected to an active load. The load current is measured by the converter, and then its value is sent to the fuel cell model. With the given load current, the corresponding fuel cell stack output voltage is computed by the fuel cell model and its value is sent back to the DC/DC converter. Then the embedded controller regulates the converter voltage to meet the desired voltage output.

Thus, with an accurate fuel cell model, a real fuel cell electrical power output behavior can be emulated. In addition, a supervisory computer with a human-machine interface is also connected to the data bus, in order to monitor the fuel cell emulator operating state and to log the test data.

B. DC/DC Buck Power Converter design

1) Fuel cell stack dynamics influence:

As mentioned in section III. , the fuel cell stack voltage output depends on the fuel cell dynamics in 3 physical domains. A dynamic time constants analysis has been discussed. It can be noticed that the thermal dynamic time constant is much bigger than those in the electrical and fluidic domains. That means that the stack voltage dynamic mostly depends on the fuel cell thermal dynamic effect. Thus, the electrical and fluidic dynamics can be neglected for the converter dynamic responses consideration. Only the thermal dynamic effect is considered in the fuel cell electrical emulator design. It means that the converter has to be able to answer 10 times faster than the reference voltage variations, that is, in less than 1 s (cutoff frequency larger than 1 Hz).

In order to achieve the desired Ballard 1.2 kW NEXA fuel

cell stack emulation performance, the converter characteristics should be:

- Converter output power: 1,200 W
- Output voltage range: from 20 V to 50 V
- Output current range: from 1 A to 50 A
- Buck converter supply voltage: 60 V DC
- PWM frequency: 10 kHz
- Converter minimum cutoff frequency: 1 Hz

A DC/DC buck converter diagram is presented below to control the power of the fuel cell emulator.

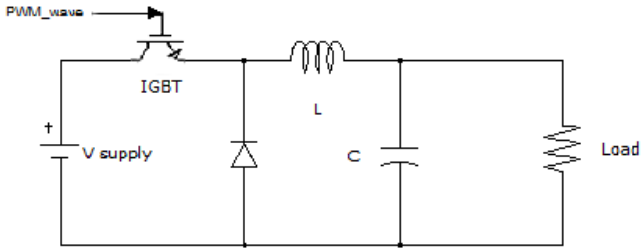

Fig. 7 DC/DC buck converter diagram

2) Converter Inductance:

The converter inductance value is calculated from the converter minimum current, in order to ensure that the converter is always working in Continuous-Conduction Mode (CCM). CCM is required for a linear operation of the converter, and the minimum current is guaranteed by the auxiliary power required to run a fuel cell.

In order to calculate the values for the output filter (inductance and capacitance) for the buck converter, the PWM (Pulse-Width Modulation) period time T_{PWM} (s), the converter supply voltage V_d (V) and the converter minimum current $I_{\min}$ (A) are required. Knowing these values, the minimum value of inductance can be obtained [12]:

$$L > \frac{T_{PWM} \cdot V_d}{8 \cdot I_{\min}} = \frac{10^{-4} \times 60}{8 \times 1} = 0.75 \cdot 10^{-3}(\mathrm{H}) \quad (19)$$

Thus, L = 1 mH is chosen for the converter.

3) Converter Capacitance:

The converter capacitance value should be chosen to meet the converter dynamic response needs. With the fixed inductance value L (H) and the converter minimum cutoff frequency $f_{c\ \min}$ (Hz), the maximum value of converter capacitance can be obtained:

$$C \le \left(\frac{1}{2\pi \cdot f_{c\min} \cdot \sqrt{L}} \right)^2 = \left(\frac{1}{2\pi\sqrt{10^{-3}}} \right)^2 = 25.33(\mathrm{F}) \quad (20)$$

On the other hand, the capacitance is also used to filter the converter output voltage ripple. Generally the DC/DC converter output voltage ripple should be less than 1 % of the output voltage:

$$\Delta V_{O\max} \le 1\% \cdot V_{O(\min)} = 0.01 \times 20 = 0.2(\mathrm{V}) \quad (21)$$

Thus the minimum capacitance value can be obtained [12]:

$$C > \frac{V_{O(\max)} \cdot {T_{PWM}}^2}{8 \cdot L \cdot \Delta V_{O\max}} = \frac{50 \cdot 10^{-8}}{8 \cdot 10^{-3} \cdot 0.2} = 312.5 \cdot 10^{-6}(\mathrm{F}) \quad (22)$$

From (20) and (22), C = 3300 µF is chosen for converter.

C. Control Strategy for DC/DC Buck Power Converter

The buck converter (IGBT switch) is controlled by a classic PI (Proportional Integral) closed loop with an anti-windup feedback. The PI loop controls the converter voltage output from the reference voltage calculated by the multi-physical model. The controller is designed in Matlab/Simulink and then implemented in a 500 µs step-size dSpace control broad. The controller diagram is presented in Fig. 8.

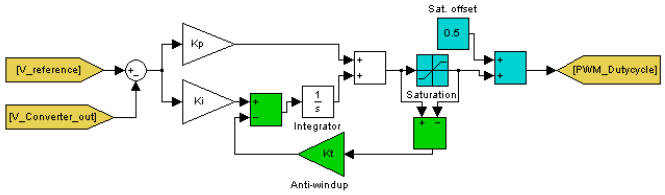

Fig. 8 Buck converter control loop

The controller coefficients, Kp, Ki and Kt (anti-windup) are adjusted during experimentation using the Ziegler-Nichols tuning rule. Their final values are listed in the table below.

TABLE I. PI CONTROLLER COEFFICIENTS

	value
Kp	0.005
Ki	1.5
Kt (anti-windup)	300

D. Experimental Validations

The DC/DC buck converter is validated by experimental tests. The converter is connected to an active load in the same test conditions with the Ballard NEXA fuel cell stack. The current profile applied to the active load is the same than the one given in Fig. 1.

Fig. 9 shows the designed DC/DC buck converter output voltage compared to the model prediction and the real stack voltages.

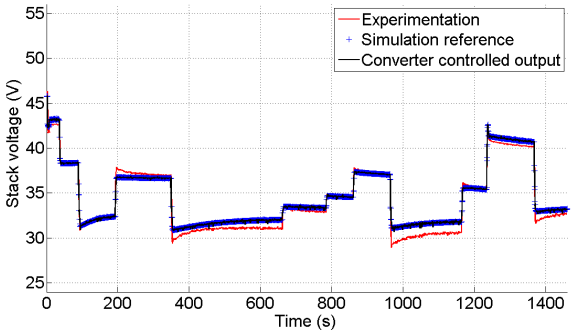

Fig. 9 DC/DC buck converter measured output voltage

From the experimental results, it can be concluded that the buck converter output voltage follows the model predicted value with a very good accuracy. In addition, the voltage of

the fuel cell emulator shows a good dynamic agreement compared to the real stack voltage curve. Thus, the real stack can be well emulated.

In order to compare more clearly between the 3 physicals values, Fig. 9 is zoomed-in from 845 s to 862 s, as shown in Fig. 10.

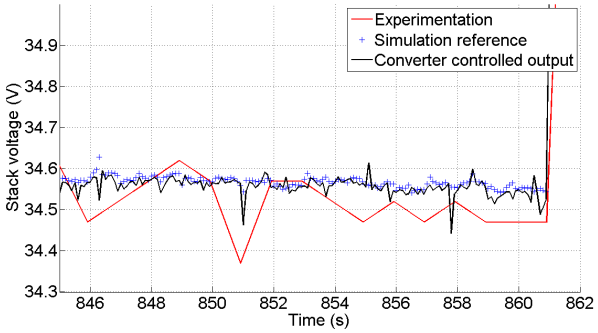

Fig. 10 Zoom-in for converter output voltage

In this figure, it can be noticed that the converter voltage ripple is largely less than 1 % of the output voltage. Thus, the design goal discussed in previous section is well achieved.

Under these test conditions, the buck converter overall efficiency is around 80%.

V. Conclusion

In this paper, a model based fuel cell emulator using a DC/DC buck converter has been presented. The fuel cell is a multi-physical system, and accurate model output can only be achieved if the model considers different physical domains. The presented real-time multi-physical fuel cell stack model covers the three major physical domains: electrical, fluidic and thermal. The model is validated for a commercial Ballard NEXA 1.2 kW fuel cell stack.

Fuel cell dynamic phenomena analysis in different physical domains have been performed and discussed. The dynamic time constants in electrical and fluidic domains are quite small compared to those in thermal domain. Therefore; the thermal response is dominant and a DC/DC buck converter must follow the dynamics imposed by the thermal part.

With the model predicted stack voltage value, the fuel cell stack power output is emulated by DC/DC buck converter. The converter is designed to meet the real fuel cell dynamic responses. The emulation results are presented and discussed. The converter output has a very good accuracy compared to the model predicted value. The converter ripple is less than 1 % at different voltage levels. Thus, the overall fuel cell emulator is validated. Such an emulator is of great interest for real time Hardware-In-the-Loop (HiL) applications.

VI. References

[1] B. Blunier and A. Miraoui, Pile à combustible (French). 2007, Paris: Ellipses. 173.

[2] F. Gao, B. Blunier, A. Miraoui, and A. E. moudni, A multiphysic dynamic 1D model of a proton exchange membrane fuel cell stack for real time simulation. IEEE Transactions on Industrial Electronics. *In press, Accepted paper*, 2009.

[3] P. Acharya, P. Enjeti, and I. J. Pitel, An Advanced Fuel Cell Simulator, in IEEE applied power electronics conference (APEC'04). 2004. p. 5.

[4] J. M. Corrêa, F. A. Farret, J. R. Gomes, and M. G. Simões, Simulation of Fuel-Cell Stacks Using a Computer-Controlled Power Rectifier With the Purposes of Actual High-Power Injection Applications. IEEE Transactions on industry applications, 2003. 39(4): p. 7.

[5] M. Ordonez, M. T. Iqbal, and J. E. Quaicoe, Development of a fuel cell simulator based in an experimentally derived model, in IEEE Canadian conference on electrical and computer engineering. 2005. p. 4.

[6] P. Acharya, P. Enjeti, and I. J. Pitel, An Advanced Fuel Cell Simulator, in IEEE applied power electronics conference (APEC'04). 2004. p. 5.

[7] T.-W. Lee, S.-H. Kim, Y.-H. Yoon, S.-j. Jang, and C.-Y. Won, A 3kW Fuel Cell Generation System using the Fuel Cell Simulator, in IEEE 35th annual power electronics specialists conference (PESC 04). 2004. p. 5.

[8] N.-A. Parker-Allotey, A. T. Bryant, and P. R. Palmer, The Application Of Fuel Cell Emulation In The Design Of An Electric Vehicle Powertrain. IEEE, 2005: p. 6.

[9] G. Marsala, M. Pucci, G. Vitale, M. Cirrincione, and A. Miraoui, A prototype of a fuel cell PEM emulator based on a buck converter. Applied Energy, 2009. *In press:* p. 12.

[10] F. Gao, B. Blunier, A. Miraoui, and A. E. moudni, Cell layer level generalized dynamic modeling of a PEMFC stack using VHDL-AMS language. International Journal of Hydrogen Energy, 2009. 34(13): p. 24.

[11] R. O'Hayre, S.-W. Cha, W. Colella, and F. B. Prinz, Fuel cell fundamentals. 1st ed. 2005: John Wiley & Sons, INC. 409.

[12] N. Mohan, T. M. Undeland, and W. P. Robbins, Power Electronics: Converters, Applications, and Design. 3rd ed. 2002: Wiley. 824.